EXPERIMENTAL AND NUMERICAL INVESTIGATION OF VIBRATION AND DAMPING PROPERTIES OF *ALSTONIA MACROPHYLLA* FIBER REINFORCED POLYPROPYLENE COMPOSITES: EFFECT OF FIBER CONCENTRATION

HARSHAVARDHAN BETTEGOWDA,[*] SHETTAHALLI MANTAIAH VINU KUMAR,[**] ERUSAGOUNDER SAKTHIVELMURUGAN,[***] RAVICHANDRAN ARUMUGAM THANGAVEL,[****] CHANDRASEKARAN SASIKUMAR[***] and SANTHOSH NAGULAN[*****]

[*]*Department of Mechanical Engineering, National Institute of Engineering, Mysuru-570008, Karnataka, India*
[**]*Department of Mechanical Engineering, Sri Krishna College of Engineering and Technology-Kuniyamuthur, Coimbatore, Tamil Nadu, India*
[***]*Department of Mechanical Engineering, Bannari Amman Institute of Technology, Sathyamangalam, Tamil Nadu, India*
[****]*Department of Mechanical Engineering, Vel Tech Rangarajan Dr Sagunthala R&D Institute of Science and Technology-Avadi, Chennai, Tamil Nadu, India*
[*****]*Department of Mechanical Engineering, Easwari Engineering College, Chennai, Tamil Nadu, India*
✉ *Corresponding author: S. M. Vinu Kumar, vinukmr1988@gmail.com*

Received October 17, 2025

Many automotive and aerospace industries have shown increasing interest in the manufacture of components from natural fiber composites due to their unique properties, such as low density, low processing cost, biodegradability, recyclability, and tailorable mechanical properties, compared to the synthetic fiber composites. In this context, *Alstonia macrophylla* (ASM) fiber reinforced polypropylene (ASM/PP) composites were fabricated using the hot-pressing technique. The main focus of this study was to investigate the effect of fiber content on the vibration and damping properties of the ASM/PP composites. ASM fiber was reinforced into PP on volume fraction basis ranging from 0 to 50 vol% in increments of 10 vol%. The resulting composites were designated as Neat PP, A10, A20, A30, A40 and A50 composites, respectively. Free vibration test results revealed that the addition of 40 vol% of ASM fiber into PP enhanced the natural frequency (Mode-I) of the composites. However, at lower fiber content, natural frequency of the ASM/PP composites was reduced due to the softening effect dominated by the PP matrix. Highest damping ratio was exhibited by A30 composites, however beyond 30 vol%, a significant drop in damping ratio was observed. This may be owing to poor agglomeration of the fibers at higher concentration. Experimental results were found to be in good agreement with numerical results obtained from Abaqus simulations, with an error limited to 2.28%. CAE models of the specimens were prepared as per their actual dimension. However, for enhancing effectiveness of the simulation results, the mass of the accelerometer was considered. FESEM analysis on the fractured surface supported the improvement in damping and stiffness properties.

Keywords: natural frequency, damping, PP composites, effective stiffness, model analysis

INTRODUCTION

Industrial utilization of plastic materials for fabricating engineering components is fuelling environmental issues, despite offering outstanding physico-mechanical properties and significant weight reduction compared to conventional materials.[1] In recent years, researchers have been highly motivated to develop new formulations of polymer composites reinforced with natural fiber (NFRPCs) due to their numerous advantages over synthetic based composites, including low density, biodegradability, recyclability, simple fabrication, easy processing, lower energy consumption *etc*.[2,3]

This approach not only tackles the environmental issues, but also enhances the mechanical properties of the NFRPCs. Many automotive interior parts, such as dashboards, door panel, backrests, and cabin elements are made from the natural fiber composites owing to their superior acoustic and thermal insulation properties. In addition to these advantages, such composites contribute to overall structural weight reduction and thereby improves fuel efficiency of the vehicle, without sacrificing overall mechanical properties of the components.[4] However, being lightweight, components made from NFRPCs are more vulnerable to audible noise and vibration. Besides, these composites are subjected to repetitive forces during service. If these forces are at regular intervals and exceed the threshold level, they may induce problems like intense vibrations, wear and tear, unwanted noises, energy loss or, in some cases, structural damage over time.[5] Therefore, understanding of the material response to these unwanted forces or vibrations is crucial to predict possible mode of failure and to enhance the composite design for higher durability.[6]

Natural fibers are viscoelastic in nature, so inherently contribute to the dissipation of the energy. On the other hand, polymers are also viscoelastic materials and exhibit more damping properties than metallic materials. Thus, embedding natural fiber in a polymer matrix can provide multifunctional performance, such as vibration control, energy and heat dissipation, along with the improved stiffness.[7,8] NFRPCs have the ability to dissipate energy by means of converting vibrational energy into heat energy during mechanical deformation and offer higher damping properties, which may be attributed to internal friction between fiber and matrix.[9] In order to understand the relationship between the damping properties and energy dissipation in the composite material system, the logarithmic decrement (δ) parameter is determined, which simply conveys the rate at which vibrational energy is dissipated within the material. Higher the values indicate more energy dissipation and stronger damping properties.[10]

Many studies have been reported on experimental investigations of NFRPCs, particularly on thermoset-based composites, with epoxy or polyester used as matrix. For example, vibrational properties of sisal/cotton reinforced polyester,[11] jute-fabric reinforced polyester,[12] flax reinforced epoxy,[13] glass/carbon hybrid reinforced epoxy,[14] banana/coconut sheath fiber reinforced polyester,[15] and banana-jute reinforced polyester composites[16] have been studied. However, thermoplastic matrices dissipate more energy, and substantially reduce amplitude and noise, compared to thermoset ones. Furthermore, the flexibility characteristic of thermoplastic helps restrict crack initiation and propagation under continuous cyclic vibration.[17,18] Amongst the thermoplastics, polypropylene is a highly appreciated matrix material. It is widely preferred for the manufacture of aerospace, automotive and consumer sector products, due to its exceptional qualities, such as low density, excellent processability, better damping ability, moisture and chemical resistance, durability, and low cost.[19] Considering its merits, a few findings on the vibrational characteristics of natural fiber reinforced polypropylene composites were reported, for instance, on sisal/polypropylene,[20] flax/polypropylene,[21] hemp woven fabric/polypropylene,[3] hemp/polypropylene[22] and wood flour/polypropylene composites.[23]

Alstonia macrophylla fiber can be extracted from the dry seeds of the plant and has been investigated elsewhere as a potential reinforcement agent in polymer composites.[24] However, no findings related to the vibration properties of *Alstonia macrophylla* fiber reinforced PP composites have been reported so far. Thus, this study aims to investigate the vibrational damping behavior of *Alstonia macrophylla* fiber reinforced PP composites as a function of fiber concentration. Experimental results were compared with numerical analysis performed using Abaqus software to confirm the effectiveness of the CAE model used.

EXPERIMENTAL

Materials

Polypropylene (PP) sheets supplied by the Ghanshyam Polyplast (Coimbatore, TN, India) were used as matrix materials. *Alstonia macrophylla* fiber, cellulosic fiber extracted from the dry seed pods, was used as a reinforcement agent in the preparation of ASM/PP composite. The procedure adopted for fiber extraction has been reported in our previous works.[26,27] The physico-mechanical and chemical properties of the *Alstonia macrophylla* fiber and polypropylene materials are shown in Figure 1.

Fabrication of ASM/PP composites

ASM/PP composites were prepared using the film stacking method, followed by hot pressing in the compression moulding machine at elevated temperature and pressure. Initially, PP sheets and ASM fibers were alternatively stacked as per the volume fraction required and placed in the aluminium mould. The entire mould assembly was then transferred to the compression moulding machine and subjected to the combined effect of pressure (25 bar) and temperature (180 °C) for a period of 15 minutes. During this compaction time, once polypropylene reaches its melting point temperature, additional pressure of 0.5 bar was applied for the duration of 5-10 seconds to enhance the adhesion of the fiber and matrix phase. Subsequently, the mould assembly was cooled to normal room temperature, after which the ASM/PP composites were removed from the mould and utilized for further studies.

The fabricated ASM/PP composites are shown in Figure 2. The composition of the ASM/PP composites with respect to the volume fraction is detailed in Table 1.

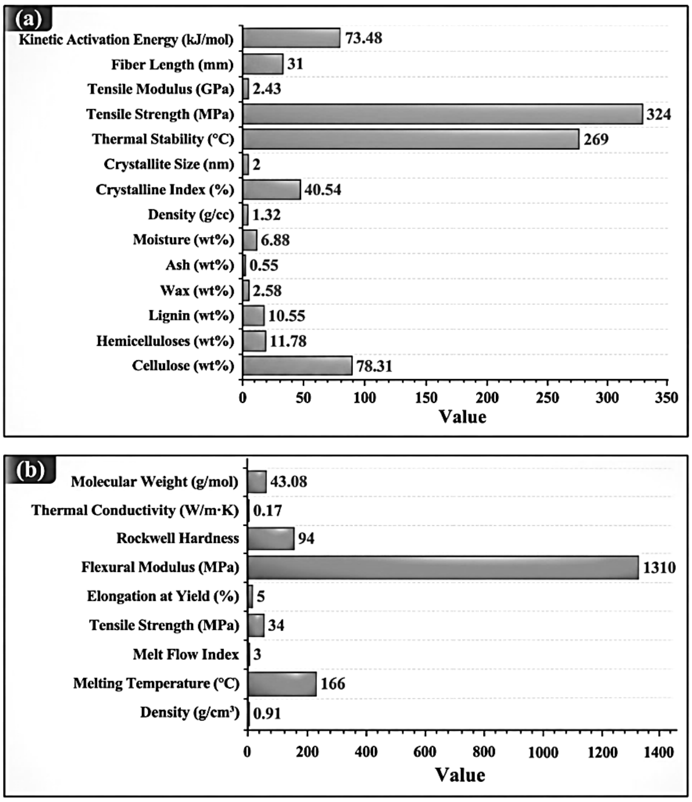

Figure 1: Physico-mechanical and chemical properties of (a) *Alstonia macrophylla* fiber and (b) polypropylene[24,25]

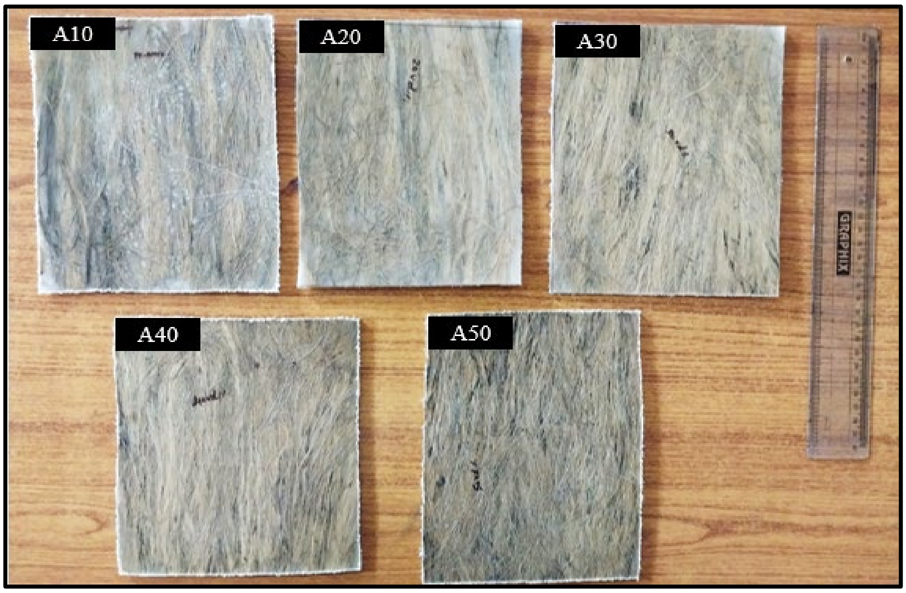

Figure 2: Fabricated ASM/PP composites

Table 1
Composition of ASM/PP composites

S. No	Composition	Volume fraction (vol%)		Density (g/cc)	Elastic modulus (GPa)
		Alstonia macrophylla fiber (vol%)	Polypropylene (vol%)		
1	PP	-	100	0.7407	1.42
2	A10	10	90	0.8544	1.78
3	A20	20	80	0.9054	1.96
4	A30	30	70	0.9463	2.08
5	A40	40	60	0.9728	2.48
6	A50	50	50	0.8543	2.23

Free vibration setup

The damping properties of the ASM/PP composites were determined by conducting the single cantilever free decaying test. The composite samples were mounted in a cantilever beam configuration, as indicated in Figure 3. For experimental assessment and numerical simulation, the effective length of the ASM/PP composite beam was considered to be 110 mm. A piezoelectric accelerometer (Model PCB 356A15) was used to record the response of the vibrating beam, and the mass accelerometer (10.5 grams) – to measure the frequency with ± 5 % accuracy.

For the measurement, firstly an accelerometer was mounted on the free end of the cantilever beam (ASM/PP composite) using temporary adhesive, as shown in Figure 3. The analogue response obtained by the accelerometer was digitalized by using an NI 9234 IEPE input module. Digitalized data was further transferred to the computer system via an NI compact data acquisition module cDAQ 9178. Finally, the received digital data was analysed using the NI Labview software package.

ASM/PP composite was vibrated by impact using a hammer. Since no viscous damper was connected, neglecting the air damping, it was presumed that vibrating ASM/PP composite beam decreases its amplitude of oscillation in each cycle and attains the equilibrium position after finite time.[27] The decrement of amplitude in every successive cycle was computed using the logarithmic decrement parameter.[13,27] It is simply the ratio of the natural logarithm of two successive amplitudes, and the logarithmic decrement of the ASM/PP composite was computed using Equation (1):

$$\delta = \frac{x_1}{x_2} = \frac{1}{n}\, ln\left(\frac{x_1}{x_{n+1}}\right) \tag{1}$$

Damping ratio (ζ) was calculated using Equation (2). Further by using Equations (3) and (4), damped (f_d) and undamped frequencies (f_n) of the single degree of freedom system were determined:

$$\zeta = \frac{\delta}{2\pi} \tag{2}$$

$$f_d = \frac{1}{2\pi}\left(\frac{n}{t}\right) \tag{3}$$

$$f_n = \frac{2\pi f_d}{\sqrt{1-\zeta^2}} \tag{4}$$

where 't' is the time taken to cover the 'n' number of cycles. By considering the point load 'M' acting at the tip of the cantilever beam system apart of the mass of the beam 'm', then natural frequency (f_n) for the single DOF can be measured by employing Equation (5):

$$f_n = \frac{1}{2\pi}\sqrt{\frac{\frac{3EI}{l^3}}{M+\frac{33}{140}m}} \tag{5}$$

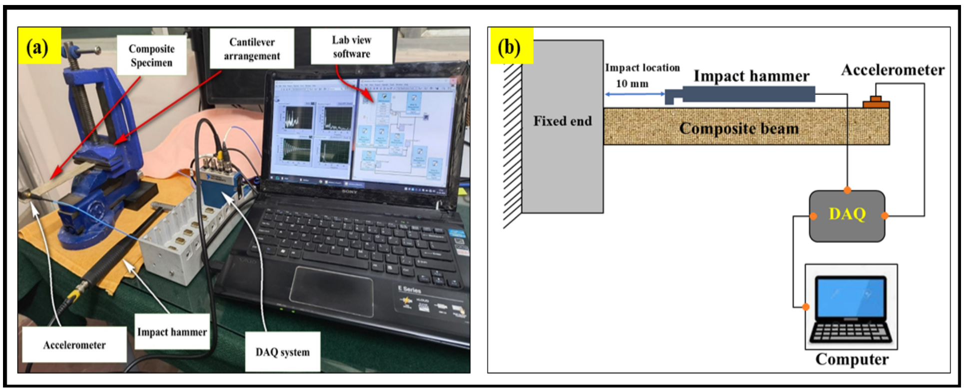

Figure 3: Experimental setup of free vibration test

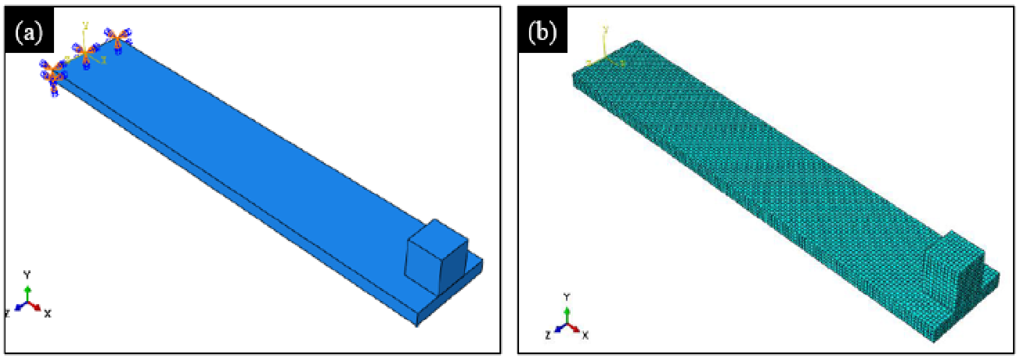

Figure 4: Geometry and mesh created for the ASM/PP composites using Abaqus software

Numerical simulation in Abaqus

Numerical simulation was performed on the ASM/PP composites to understand their anisotropic behaviour during vibration. Finite elemental type numerical modal analysis was performed using Abaqus CAE 2017 software package. The mass of the accelerometer (whose density was 4560 kg/m^3) was considered for performing the modal analysis. The geometry of the ASM/PP composite beam was modelled as per its actual dimension, and the interaction between the composite beam and the sensor was established as shown in Figure 4. The ASM/PP composite beam was assumed to be a homogenous material for numerical analysis. The tensile modulus of the composite materials was experimentally obtained and used as an input material.[27,28] Since excitation was applied on a cantilever beam, one end of the geometry was fixed, therefore constraining all DOF at that end. Geometries were meshed with C3D8R elements, as shown in Figure 4, and a linear frequency perturbation analysis was subsequently performed.

FESEM analysis

The fractography analysis of ASM/PP composites was performed using Field Emission Scanning Electron Microscopy (FESEM) (Carl Zeiss Sigma 300, Germany).

RESULTS AND DISCUSSION

Vibration decay curves of the various ASM/PP composites are depicted in Figure 5. These curves help understand the energy dissipation by the composite material over time and reveals their true damping characteristics. From the curves, it is clearly observed that the neat PP laminate exhibits the lowest damping as amplitude decays slowly. However, vibration seems to persist longer, indicating an elastic response. A slight improvement in the damping is shown by the A10 composites, whose amplitude decays faster than for PP, which may be due to the strong fiber-matrix interaction. Further addition of 20 vol% and 30 vol% ASM fiber into the PP matrix has strengthened the damping behaviour of the ASM/PP composites, with notable faster decay time, suggesting better interfacial energy dissipation. Higher damping is exhibited by the A30 composite whose amplitude decays faster than for A20 composite, as shown in Figure 5. In contrast, at higher fiber loading, the A40 composite struggles to exhibit better damping property and the curve clearly shows that the amplitude decay is slower than for the A30 composite, which may be attributed to the poor interfacial bonding or fiber agglomeration. Further addition of 50vol% ASM fiber to the PP (A50 composite) showed better damping property than A40, however lower than A30 composite, implying that higher fiber loading reduces the damping efficiency of the ASM/PP composite. The amplitude decay curve of the A50 composite is similar to that of the A40 composite, which clearly conveys that vibration continues for a longer time than for other composites. Free vibration test results of the ASM/PP composite are shown in Table 2. The time periods of the vibration for neat PP, A10, A20, and A30 composites are 0.0497, 0.0567, 0.0721 and 0.0605 seconds respectively, which clearly helps understand the stiffness property of the material. A lower time period means higher stiffness and *vice-versa*. The stiffness of the composites decreases with the increase in the fiber loading up to 30 vol%, which clearly enhanced the damping property of the ASM/PP composites. However, from Table 2, it is evident that the addition of higher fiber loading helps regain the material's stiffness property. Particularly A40 and A50 composites exhibit higher stiffness property than PP, as their vibration time period lasted for 0.0460 and 0.0467 seconds, which clearly shows that the material suffers from reduced damping property at higher loading, which is in consistency with the results observed from the amplitude–time curves.

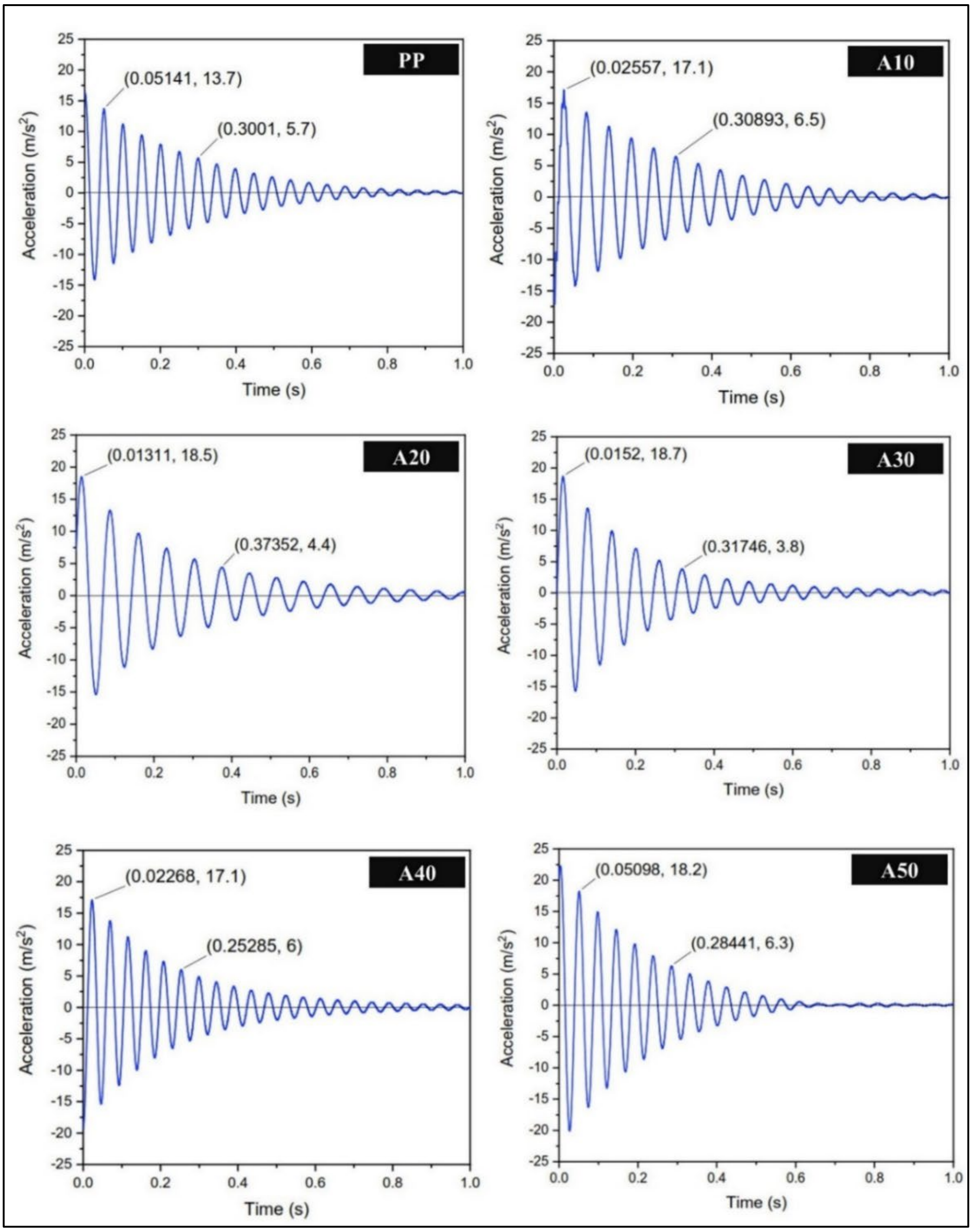

Figure 5: Amplitude of vibration of ASM/PP composites in the time domain

This is explained by the fact that, at higher fiber loading, interfacial bonding deteriorated and poor fiber–matrix adhesion accompanied by higher voids leads to a decrease in energy transfer efficiency, eventually resulting in lower damping property. Consequently, the composites become stiffness dominated rather than damping dominated. The vibrational damping behaviour of the ASM/PP composites was examined under the influence of varying fiber content. The composite specimens of 140 mm in length, under cantilever beam configuration, were impacted by the hammer at three equidistant points. The obtained force and displacement signals were further processed using MATLAB (R2021) software, the amplitudes of the curves in the frequency and time domains were illustrated in Figure 5 and Figure 6, respectively. Natural frequencies of the ASM/PP composites were obtained in the range of 14 to 22 Hz, as shown in Figures 6 and 7. Neat PP exhibited a natural frequency of 20.48 Hz, whereas composites A10, A20 and A30 recorded lower natural frequencies than neat PP, despite the increasing fiber concentration. This may be due to non-uniform stiffness distribution caused by the fiber and the increase in the mass density of the composite material. This reduction may also have occurred because of the softening effect dominated by the matrix phase. However, further addition of ASM fiber improved the natural frequencies of the ASM/PP composites. A40 and A50 composites exhibited higher natural frequency than other composites, which is mainly attributed to the increase in the stiffness of the composites. Similar observations were reported by other researchers.[3,20,22] From Figure 8, it is evident that increasing the ASM fiber content in the PP phase has improved the damping property of the composites, which may be due to the increased viscoelastic dissipation from the fiber-matrix interface.[26,28,29] Maximum damping ratio is exhibited by the A30 composites (0.0507), which implies that, at this optimum fiber content (30 vol%), the interfacial adhesion is more effective and participated in absorbing higher vibrational energy. Moreover, higher damping ratios of the composite material also suggests that mechanisms such as microstructural dissipation and internal friction at the fiber-matrix interface effectively contributed to higher internal damping. However, the addition of fiber beyond 30 vol% led to a significant drop in damping behavior, as shown in Figure 8. This may be ascribed to fiber agglomeration, resulting in poor interfacial bonding, which ultimately affects the energy dissipation and thus, the damping property. Furthermore, the behavior of the *Alstonia macrophylla* fiber is elastic, whereas the property of the PP matrix is viscoelastic in nature. Increasing the fiber loading transforms the material's behavior from viscoelastic to elastic, which ultimately results in reducing the damping ratio.[20]

Figure 9 shows the relationship between the density and relative stiffness of the ASM/PP composites. From the plot, it is clear that the density of the ASM/PP composites steadily increases with the increase in the fiber content, up to 40 vol%, and then decreases. This may be due to the presence of an equal proportion of fiber and matrix, causing differences in porosity. Overall, A10, A20, A30, A40 and A50 composites are heavier than neat PP. The effective stiffness (E) of the neat PP is 1. The addition of fiber from 10 vol% to 30 vol% decreases the E value lower than 1 and so frequency drops. A10, A20, and A30 displayed E values of 0.87, 0.60 and 0.82, respectively, despite increased density. This clearly indicates poor load transfer, weaker fiber–matrix bonding and intense fiber compaction, while fabrication reduces the effective modulus.[30] A40 and A50 composites showed higher E values of 1.49 and 1.23, compared to the other composites.

Table 2
Free vibrational test results of ASM/PP composites

Parameters \ ASM/PP Composites	PP	A10	A20	A30	A40	A50
Time, t_1 (s)	0.0514	0.0256	0.0131	0.0152	0.0227	0.051
Time, t_2 (s)	0.3001	0.3089	0.3735	0.3175	0.2529	0.2844
Acceleration, a_1 (m/s^2)	13.7	17.1	18.5	18.7	17.1	18.2
Acceleration, a_2 (m/s^2)	5.7	6.5	4.4	3.8	6	6.3
Logarithmic decrement	0.175	0.193	0.287	0.319	0.209	0.212
Damping ratio (ς)	0.0279	0.0308	0.0457	0.0507	0.0333	0.0338
Time period (s)	0.0497	0.0567	0.0721	0.0605	0.046	0.0467
Damped frequency (Hz)	20.11	17.65	13.87	16.54	21.72	21.42
Undamped frequency (Hz)	20.48	17.75	14.34	16.38	21.85	21.16
Density of beam material (kg/m^3)	884	850	910	950	980	940
Mass of beam, M_β (kg)	0.01238	0.01233	0.0099	0.01033	0.01066	0.01363
Mass of transducer, M_t (kg)	0.0105	0.0105	0.0105	0.0105	0.0105	0.0105
Effective mass, M (kg)	0.01342	0.013405	0.012833	0.012935	0.013012	0.013713
Tensile modulus (GPa)	1.42	1.78	1.96	2.08	2.48	2.23

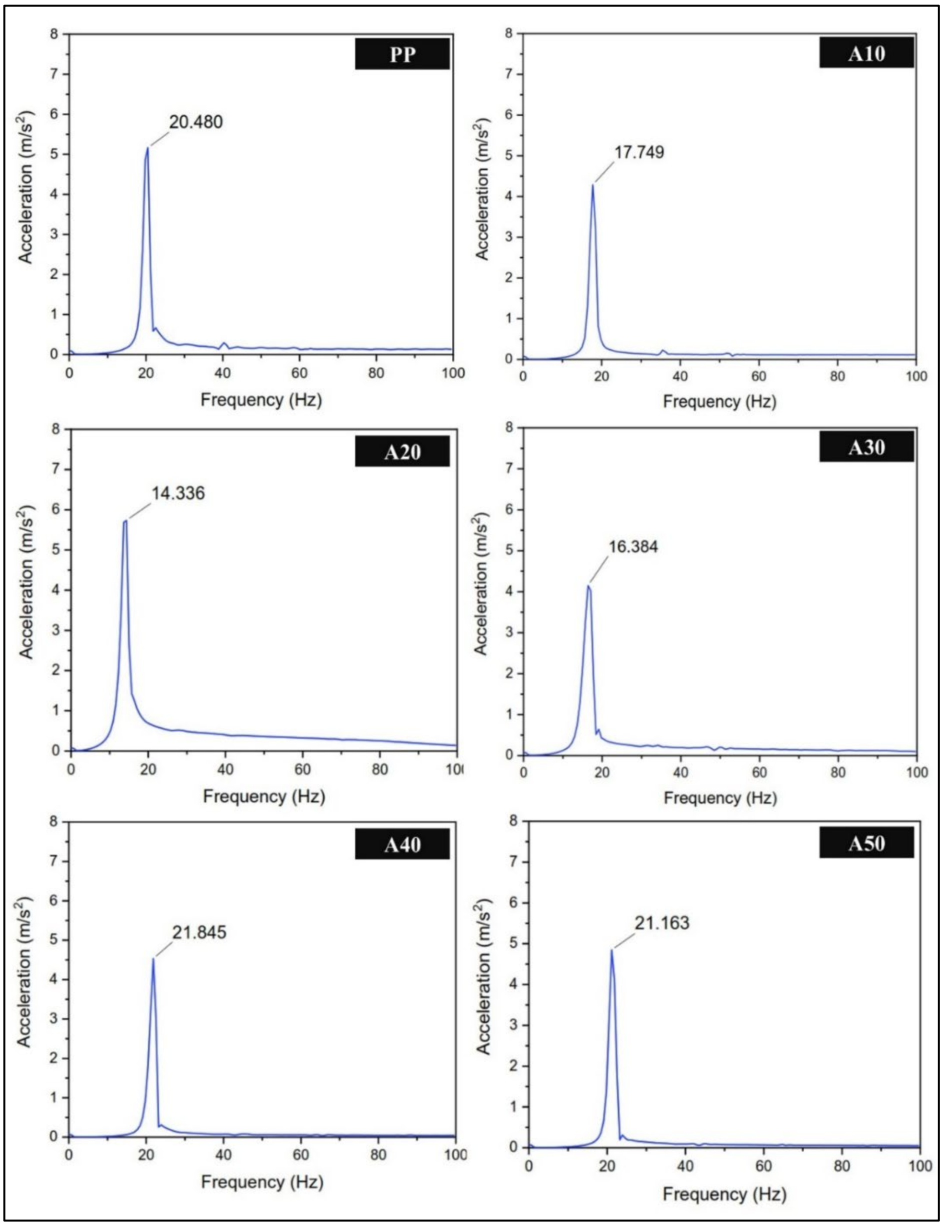

Figure 6: Amplitude of vibration of ASM/PP composites in the frequency domain

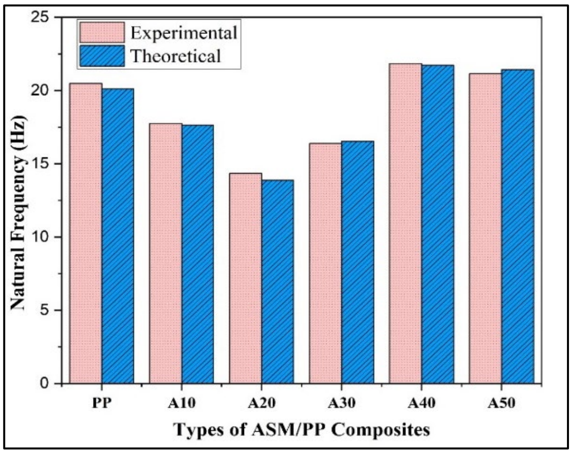

Figure 7: Natural frequency (Mode-I) of ASM/PP composites

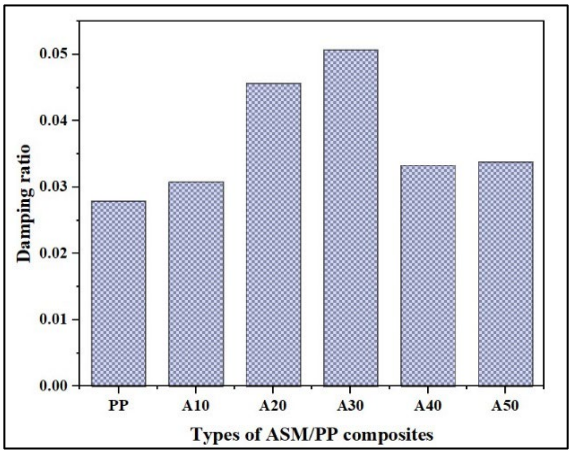

Figure 8: Damping ratio of ASM/PP composites

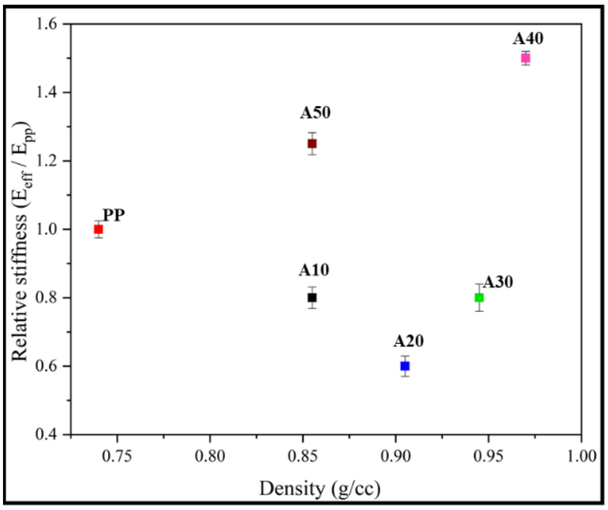

Figure 9: Relation between density and relative stiffness of ASM/PP composites

Significantly higher E value was recorded, suggesting that the regain of stiffness dominates and frequency increases over that of the neat PP. At higher fiber loading, there is an enhanced fiber continuity, and so the load bearing ability dominates, which eventually leads to improved stiffness, even at higher mass, which is consistent with the previous discussion on the natural frequency of the composites. Overall, the natural frequency of the ASM/PP composites is governed by the combined effect of density and effective stiffness (E).

Numerical simulation

Figure 10 shows the numerically simulated mode-I shape of the ASM/PP composite beam. As discussed before, the accelerometer mounted on the composite beam is clearly indicated in the plot. From the simulated results, it is clear that the pattern of deformation is consistent with the anticipated first bending mode. Numerical frequencies of the ASM/PP composites are in close agreement with the experimental results with the minimum error percentage between 0.25% to 2.28%, as shown in Table 3, indicating the reliability and efficacy of the finite model. Though the experimental and simulation results are found to be consistent, still there is a slight deviation, which is inevitable, as this may be attributed to the damping effect caused by the air resistance during testing. In addition, factors such sensor mass influence, material properties, and boundary conditions are also accountable for the discrepancies between simulated and experimental results.

The obtained findings are in line with the results reported by Harshavardhan *et al*.[31] They reported an error between numerical and experimental results in the range of 5.0% for short carbon fiber reinforced polyethersulfone composite. They confirmed that the inclusion of viscoelastic material model in the numerical simulation gave an accurate representation of the material's behaviour and thus helped minimize the error between experimental and natural frequencies. Moreover, mesh refining and the incorporation of realistic damping parameters will also improve the effectiveness of the numerical simulation.

Table 3
Experimental and simulated natural frequencies of ASM/PP composites

S. No	Sample	Natural undamped frequency (Hz)		Error (%)
		Experimental	Simulated	
1	PP	20.48	20.693	1.04
2	A10	17.75	17.901	0.85
3	A20	14.34	14.667	2.28
4	A30	16.38	16.506	0.77
5	A40	21.85	21.905	0.25
6	A50	21.16	21.298	0.66

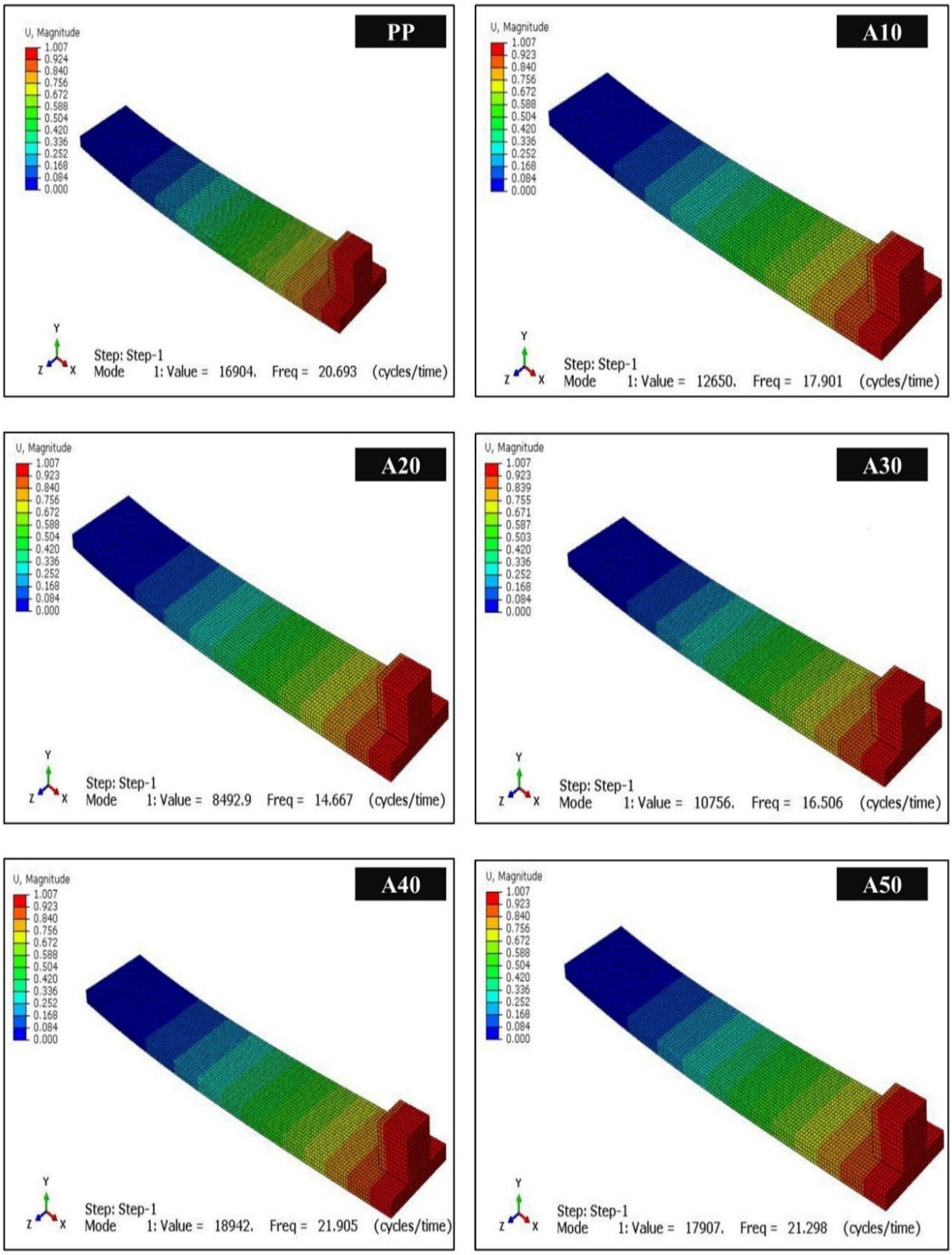

Figure 10: Abaqus simulated frequencies of ASM/PP composites

FESEM analysis

Free vibration test specimens of ASM/PP composites did not experience any fracture. FESEM observations were carried out for examining the fractured surface of the tensile tested composites from the same batch. During numerical simulation, tensile modulus values were introduced as input data to determine the natural frequencies of the composite materials. This approach paves the way for better understanding of the microstructural mechanisms impacting both elastic and dynamic responses of the ASM/PP composites.

FESEM images of the tensile fractured surface of the A30 and A40 composites are shown in Figure 11. The fractured surface of the A40 composites clearly revealed the fiber–matrix interactions, exhibiting strong interfacial adhesion and lesser voids, indicating the cohesive fractured surface, which is in line with the higher tensile modulus (2.48 GPa) and natural frequency (21.85 Hz) observed in the free vibration test. In contrast, the fractured surface of the A30 composites showed significant fiber pull-outs and delamination, along with the localized interfacial gaps, clearly suggesting lower stiffness and higher damping property of the composites. This may be ascribed to increased interfacial frictional energy dissipation.

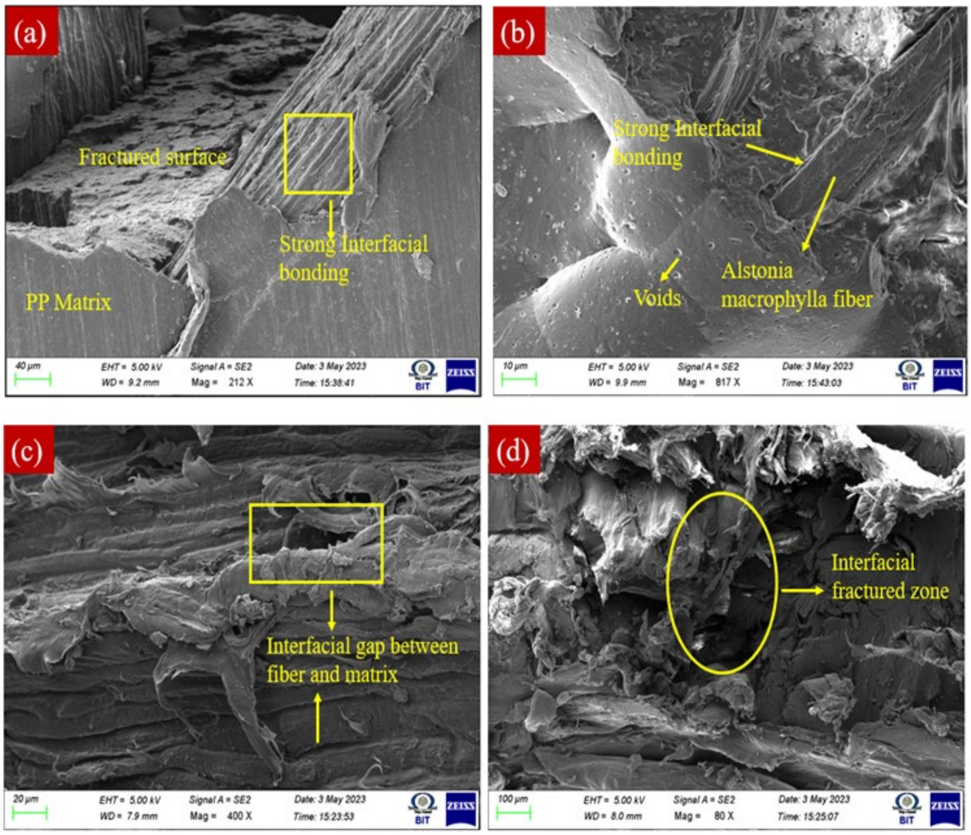

Figure 11: Fractured surfaces of ASM/PP composites

CONCLUSION

In this study, polypropylene composites reinforced with ASM fibers, at different volume fraction, were successfully manufactured and their vibration and damping behaviours were investigated. The experimental results allowed drawing the following conclusions:

- Amongst the tested composites, the A40 composite exhibited the highest natural frequency value (21.85 Hz), followed by the A50 composites. However, neat PP showed better natural frequency than A10, A20 and A30 composites. This may be due to the softening effect dominated by the matrix and non-uniform stiffness distribution caused by the reinforcement agent.

- The damping ratio of the ASM/PP composites increased with the increase in the fiber content. The highest damping ratio was demonstrated by A30 composites, followed by A20. The damping property of the ASM/PP composites was demonstrated by establishing the relationship between density and effective stiffness of the material, normalized with respect to the PP content.

- Experimental results of the natural frequencies of ASM/PP composites were found to be in good agreement with simulated results obtained from Abaqus simulation, with a maximum error of 2.28%, which clearly conveys the effectiveness of the Abaqus CAE model employed.

- Fractography analysis carried out using FESEM clearly revealed fiber–matrix bonding, void content and delamination, which is agreement with the damping property of the ASM/PP composites.

REFERENCES

[1] S. Antony, A. Cherouat and G. Montay, *Polym. Polym. Compos.*, **29**, 175 (2021), https://doi.org/10.1177/09673911211023942

[2] R. Rajiev, S. V. Kumar, H. Singh and E. Sakthivelmurugan, *Indian J. Fibre Text. Res.*, **48**, 450 (2023), https://doi.org/10.56042/ijftr.v48i4.7640

[3] P. Wambua, J. Ivens and I. Verpoest, *Compos. Sci. Technol.*, **63**, 125 (2003), https://doi.org/10.1016/S0266-3538(03)00096-4

[4] A. Bismarck, A. Baltazar-Y-Jimenez and K. Sarikakis, *Environ. Dev. Sustain.*, **8**, 445 (2006), https://doi.org/10.1007/s10668-005-8506-5

[5] V. Pinzaru, C. Bujoreanu and O. Barat, *Machines*, **12**, 862 (2024), https://doi.org/10.3390/machines12120862

[6] E. Njim, S. Bakhy and M. Al-Waily, *Arch. Mater. Sci. Eng.*, **111**, 210 (2021)

[7] F. Duc, P. Bourban and J.-A. Månson, *Compos. Sci. Technol.*, **102**, 41 (2014), https://doi.org/10.1016/j.compscitech.2014.07.004

[8] F. Duc, P.-E. Bourban, C. Plummer and J.-A. Månson, *Compos. Part A: Appl. Sci. Manuf.*, **64**, 70 (2014), https://doi.org/10.1016/j.compositesa.2014.04.016

[9] R. F. Gibson, *Compos. Struct.*, **92**, 2793 (2010), https://doi.org/10.1016/j.compstruct.2010.05.003

[10] P. Acharya, P. Dayananda and S. Hegde, *Mater. Res. Express*, **12**, 125 (2025), https://doi.org/10.1088/2053-1591/adc22a

[11] T. Sathishkumar, J. Naveen, P. Navaneethakrishnan, S. Satheeshkumar and N. Rajini, *J. Ind. Text.*, **47**, 1880 (2017), https://doi.org/10.1177/1528083716648764

[12] M. Rajesh and J. Pitchaimani, *Compos. Struct.*, **163**, 302 (2017), https://doi.org/10.1016/j.compstruct.2016.12.046

[13] S. M. V. Kumar, R. Jeyakumar, N. Manikandaprabu and C. Sasikumar, *Cellulose Chem. Technol.*, **58**, 745 (2024), https://doi.org/10.35812/CelluloseChemTechnol.2024.58.74

[14] D. Biswas and C. Ray, *J. Vib. Control*, **23**, 1372 (2017), https://doi.org/10.1177/1077546315592766

[15] K. S. Kumar, I. Siva, N. Rajini, J. W. Jappes and S. Amico, *Mater. Des.*, **90**, 508 (2016), https://doi.org/10.1016/j.matdes.2015.11.051

[16] M. Rajesh and J. Pitchaimani, *Polym. Compos.*, **39**, 1840 (2018), https://doi.org/10.1002/pc.24234

[17] U. K. Vaidya and K. Chawla, *Int. Mater. Rev.*, **53**, 185 (2008), https://doi.org/10.1179/174328008X32522

[18] M. Z. Rahman and H. Xu, *Polymers*, **15**, 1042 (2023), https://doi.org/10.3390/polym15041042

[19] Q. T. Shubhra, A. M. Alam and M. A. Quaiyyum, *J. Thermoplast. Compos. Mater.*, **26**, 362 (2013), https://doi.org/10.1177/0892705711428659

[20] Y. S. Munde, R. B. Ingle and I. Siva, *Noise Vib. Worldwide*, **50**, 108 (2019), https://doi.org/10.1177/0957456518812784

[21] M. Z. Rahman, K. Jayaraman and B. R. Mace, *Fibers Polym.*, **18**, 1565 (2017), https://doi.org/10.1007/s12221-017-7418-y

[22] A. Etaati, S. A. Mehdizadeh, H. Wang and S. Pather, *J. Reinf. Plast. Compos.*, **33**, 330 (2014), https://doi.org/10.1177/0731684413512228

[23] S. Chauhan, A. Karmarkar and P. Aggarwal, *J. Appl. Polym. Sci.*, **114**, 2656 (2009), https://doi.org/10.1002/app.30718

[24] E. Sakthivelmurugan, G. Senthilkumar, S. Kumar and H. Singh, *Cellulose Chem. Technol.*, **55**, 345 (2023), https://doi.org/10.35812/CelluloseChemTechnol.2023.57.35

[25] S. M. V. Kumar, J. Rengaraj and E. Sakthivelmurugan, *Cellulose Chem. Technol.*, **58**, 547 (2024), https://doi.org/10.35812/CelluloseChemTechnol.2024.58.51

[26] E. Sakthivelmurugan, G. Senthil Kumar, S. Vinu Kumar and H. Singh, *J. Braz. Soc. Mech. Sci. Eng.*, **45**, 8339 (2023), https://doi.org/10.1007/s40430-023-04339-y

[27] E. Sakthivelmurugan, G. Senthil Kumar and S. V. Kumar, *Mater. Res.*, **26**, 108 (2023), https://doi.org/10.1590/1980-5373-MR-2023-0108

[28] X. Tang and X. Yan, *J. Ind. Text.*, **49**, 693 (2020)

[29] R. Chandra, S. P. Singh and K. Gupta, *J. Sound Vib.*, **262**, 475 (2003)

[30] B. Harshavardhan, R. Ravishankar, B. Suresha and S. Srinivas, *IOP Conf. Ser.: Mater. Sci. Eng.*, **1185,** 012050 (2021)

[31] B. Harshavardhan, R. Ravishankar, B. Suresha and U. A. C. Dixit, *IOP Conf. Ser.: Mater. Sci. Eng.*, **1185**, 012051 (2021)